Space-Time Finite Integration Method for Electromagnetic Field Computation

AUTHOR(S):

Matsuo, Tetsuji

CITATION:

Matsuo, Tetsuji. Space-Time Finite Integration Method for Electromagnetic Field Computation. IEEE Transactions on Magnetics 2011, 47(5): 1530-1533

ISSUE DATE:

2011-04-21

URL:

http://hdl.handle.net/2433/226609

Space-Time Finite Integration Method for Electromagnetic Field Computation

Tetsuji Matsuo, *Member, IEEE,*

***Abstract*—A finite integration method on a four-dimensional space-time grid is studied for the computation of electromagnetic wave propagation, where a non-uniform time-step distribution is naturally introduced. A dual grid based on the Hodge duality and the Lorentz metric is proposed to provide a simple constitutive equation for electromagnetic variables. An explicit time-marching scheme for a non-uniform space-time grid achieves a more efficient electromagnetic field computation than the conventional FDTD method.**

***Index Terms*—Finite integration method, Hodge dual grid, Lorenz metric, space-time grid.**

I. Introduction

THE FINITE difference time domain (FDTD) method [1] requires brick-type representation of analyzed objects, whereas the finite integration (FI) method [2], [3] can use flexible spatial grids. However, both conventional FDTD and FI methods use a uniform time-step. The time-step is restricted by the Courant-Friedrichs-Lewy (CFL) condition based on the smallest spatial grid size. The FDTD method using sub-grids [4], [5] allows non-uniform time-steps, but uses only brick-type spatial grids.

In contrast, space and time are handled in a unified manner by the special theory of relativity [6]. Even when electromagnetic field computation requires no relativity theory, electromagnetic fields can be analyzed in space-time because the Maxwell equations are unaffected by the special theory of relativity. In fact, several space-time finite element methods [7]-[9] have been proposed for eddy-current analysis.

Previous work [10] introduced a space-time FI method that achieves non-uniform time-steps naturally on three-dimensional (3D) space-time grid with 2D space. This study extends the space-time FI method to a 4D space-time grid.

II. Finite Integration Method on a Space-Time Grid

A. Maxwell Equations in Space-Time

The coordinate system is denoted by:

$$(ct, x, y, z) = (x^0, x^1, x^2, x^3) \tag{1}$$

where

$$c = 1/\sqrt{\varepsilon_0 \mu_0} \tag{2}$$

and ε_0 and μ_0 are the electric and magnetic constants.

T. Matsuo is with the Department of Electrical Engineering, Graduate School of Engineering, Kyoto University, Kyoto, 615-8510 Japan, e-mail: tmastuo@kuee.kyoto-u.ac.jp

The Maxwell equations are given as [11]:

$$\mathrm{d}F = 0\ ,\ \mathrm{d}G = J \tag{3}$$

$$\begin{aligned} F &= -\sum_{i=1}^{3} E_i \mathrm{d}x^0 \mathrm{d}x^i + \sum_{j=1}^{3} \mathcal{B}_j \mathrm{d}x^k \mathrm{d}x^l, \\ G &= \sum_{i=1}^{3} H_i \mathrm{d}x^0 \mathrm{d}x^i + \sum_{j=1}^{3} \mathcal{D}_j \mathrm{d}x^k \mathrm{d}x^l, \\ J &= c\rho \mathrm{d}x^1 \mathrm{d}x^2 \mathrm{d}x^3 - \sum_{j=1}^{3} J_j \mathrm{d}x^0 \mathrm{d}x^k \mathrm{d}x^l \end{aligned} \tag{4}$$

where $(\mathcal{B}_1, \mathcal{B}_2, \mathcal{B}_3) = c\boldsymbol{B}$, $(\mathcal{D}_1, \mathcal{D}_2, \mathcal{D}_3) = c\boldsymbol{D}$, and ρ is the electric charge density: (j, k, l) is a cyclic permutation of (1, 2, 3).

The integrated form of (3) is given as:

$$\oint_{\partial\Omega_\mathrm{p}} F = 0\ ,\ \oint_{\partial\Omega_\mathrm{d}} G = \int_{\Omega_\mathrm{d}} J \tag{5}$$

where Ω_p and Ω_d are hypersurfaces in space-time; their boundaries $\partial\Omega_\mathrm{p}$ and $\partial\Omega_\mathrm{d}$ are represented by the faces of primal and dual grids in the FI method. The electromagnetic variables are defined in the FI method as:

$$f = \int_{\mathrm{S_p}} F\ ,\ g = \int_{\mathrm{S_d}} G \tag{6}$$

where $\mathrm{S_p}$ and $\mathrm{S_d}$ are the faces of primal and dual grids.

When an orthogonal space-time primal grid and its dual grid are used, the variables (6) are written as:

$$\begin{aligned} e_i &= \int_{\mathrm{Sp}} E_i \mathrm{d}x^0 \mathrm{d}x^i, b_j = \int_{\mathrm{Sp}} \mathcal{B}_j \mathrm{d}x^k \mathrm{d}x^l, \\ h_i &= \int_{\mathrm{Sd}} H_i \mathrm{d}x^0 \mathrm{d}x^i, d_j = \int_{\mathrm{Sd}} \mathcal{D}_j \mathrm{d}x^k \mathrm{d}x^l, (i, j = 1, 2, 3) \end{aligned} \tag{7}$$

where (j, k, l) is a cyclic permutation of (1, 2, 3). These variables are numbered according to the spatial center positions of faces as:

$$\begin{aligned} e^n_{1,i,j,k} &= e_1(n\Delta x^0, i\Delta x^1, (j-1/2)\Delta x^2, (k-1/2)\Delta x^3), \\ e^n_{2,i,j,k} &= e_2(n\Delta x^0, (i-1/2)\Delta x^1, j\Delta x^2, (k-1/2)\Delta x^3), \\ e^n_{3,i,j,k} &= e_3(n\Delta x^0, (i-1/2)\Delta x^1, (j-1/2)\Delta x^2, k\Delta x^3), \\ b^n_{1,i,j,k} &= b_1(n\Delta x^0, (i-1/2)\Delta x^1, j\Delta x^2, k\Delta x^3), \\ b^n_{2,i,j,k} &= b_2(n\Delta x^0, i\Delta x^1, (j-1/2)\Delta x^2, k\Delta x^3), \\ b^n_{3,i,j,k} &= b_3(n\Delta x^0, i\Delta x^1, j\Delta x^2, (k-1/2)\Delta x^3) \end{aligned} \tag{8}$$

where the center positions of S_p are indicated in parentheses in (8). The variables d_i and h_i are numbered in the same way as e_i and b_i. Hence, (5) is rewritten as:

$$d^{n+1/2}_{m,i,j,k} = d^{n-1/2}_{m,i,j,k} + \boldsymbol{C}_{\mathrm{d}m}\boldsymbol{h}^{n}_{i,j,k},$$
$$b^{n+1}_{m,i,j,k} = b^{n}_{m,i,j,k} - \boldsymbol{C}_{\mathrm{p}m}\boldsymbol{e}^{n+1/2}_{i,j,k}, (m = 1, 2, 3) \quad (9)$$

where

$$\boldsymbol{C}_{\mathrm{p}1}\boldsymbol{p}_{i,j,k} = p_{3,i,j+1,k} - p_{3,i,j,k} - p_{2,i,j,k+1} + p_{2,i,j,k},$$
$$\boldsymbol{C}_{\mathrm{p}2}\boldsymbol{p}_{i,j,k} = p_{1,i,j,k+1} - p_{1,i,j,k} - p_{3,i+1,j,k} + p_{3,i,j,k},$$
$$\boldsymbol{C}_{\mathrm{p}3}\boldsymbol{p}_{i,j,k} = p_{2,i+1,j,k} - p_{2,i,j,k} - p_{1,i,j+1,k} + p_{1,i,j,k},$$
$$\boldsymbol{C}_{\mathrm{d}1}\boldsymbol{p}_{i,j,k} = p_{3,i,j,k} - p_{3,i,j-1,k} - p_{2,i,j,k} + p_{2,i,j,k-1},$$
$$\boldsymbol{C}_{\mathrm{d}2}\boldsymbol{p}_{i,j,k} = p_{1,i,j,k} - p_{1,i,j,k-1} - p_{3,i,j,k} + p_{3,i-1,j,k},$$
$$\boldsymbol{C}_{\mathrm{d}3}\boldsymbol{p}_{i,j,k} = p_{2,i,j,k} - p_{2,i-1,j,k} - p_{1,i,j,k} + p_{1,i,j-1,k} \quad (10)$$

These result in the conventional FDTD scheme.

When a non-orthogonal primal grid and its dual grid are used, the variables (6) are rewritten as:

$$f = \int_{\mathrm{Sp}} F = S_{\mathrm{p}}(-\sum_{i=1}^{3} n_{\mathrm{p}0i}E_i + \sum_{j=1}^{3} n_{\mathrm{p}kl}\mathcal{B}_j),$$
$$g = \int_{\mathrm{Sd}} G = S_{\mathrm{d}}(\sum_{i=1}^{3} n_{\mathrm{d}0i}H_i + \sum_{j=1}^{3} n_{\mathrm{d}kl}\mathcal{D}_j) \quad (11)$$

where (j, k, l) is a cyclic permutation of (1, 2, 3) and

$$S_{\mathrm{p}} = \int_{\mathrm{Sp}} \mathrm{d}S, S_{\mathrm{d}} = \int_{\mathrm{Sd}} \mathrm{d}S,$$
$$S_{\mathrm{p}ij} = \int_{\mathrm{Sp}} \mathrm{d}x^i\mathrm{d}x^j, S_{\mathrm{d}ij} = \int_{\mathrm{Sd}} \mathrm{d}x^i\mathrm{d}x^j,$$
$$n_{\mathrm{p}ij} = S_{\mathrm{p}ij}/S_{\mathrm{p}}\ ,\ n_{\mathrm{d}ij} = S_{\mathrm{d}ij}/S_{\mathrm{d}}\ ,\ (i, j = 0, 1, 2, 3). \quad (12)$$

B. Hodge Dual Grid for Constitutive Equation

The variables f and g contain both electric and magnetic field variables. To relate f to g, the dual grid is constructed in vacuum so as to satisfy:

$$n_{\mathrm{d}0j} = n_{\mathrm{p}kl}\ ,\ n_{\mathrm{d}kl} = -n_{\mathrm{p}0j}\ ,\ (j = 1, 2, 3) \quad (13)$$

where (j, k, l) is a cyclic permutation of (1, 2, 3). Thereby,

$$f = Z_0 S_{\mathrm{p}} g/S_{\mathrm{d}} \quad (14)$$

where $Z_0 = \sqrt{\mu_0/\varepsilon_0}$ is the impedance in a vacuum. The relationships of (13) and (14) result from $F = Z_0 * G$ where * is the Hodge operator based on the Lorentz metric. The dual grid given by (13) is called the Hodge dual grid in this paper.

Fig. 1(a) illustrates the primal face with $S_{\mathrm{p}}n_{\mathrm{p}12}$ = 1, $S_{\mathrm{p}}n_{\mathrm{p}02}$ = 1/2 and no other components of $S_{\mathrm{p}}n_{\mathrm{p}ij}$, where the rotational arrows indicate the directions of the surfaces. Fig. 1(b) depicts the dual face with $S_{\mathrm{d}}n_{\mathrm{d}03}$ = 1, $S_{\mathrm{d}}n_{\mathrm{p}31} = -1/2$ and no other components of $S_{\mathrm{d}}n_{\mathrm{d}ij}$, which satisfy (13). The projections of those faces on the x^0-x^1 plane are illustrated in Fig. 1(c), which shows the orthogonality of the two faces by the Lorentz metric as discussed in [10]. Fig. 2 illustrates the primal and dual faces with $S_{\mathrm{p}}n_{\mathrm{p}23}$ = 1, $S_{\mathrm{p}}n_{\mathrm{p}31} = -1/2$ and no other components of $S_{\mathrm{p}}n_{\mathrm{p}ij}$, where the directions of the dual faces

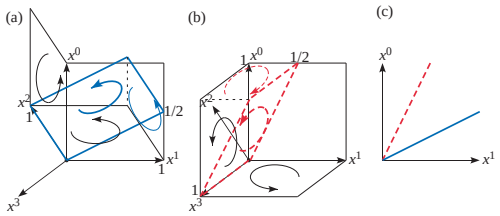

Fig. 1. Faces of primal and dual grids based on Hodge duality (13): (a) primal face, (b) dual face, and (c) the projections on the x^0-x^1 plane.

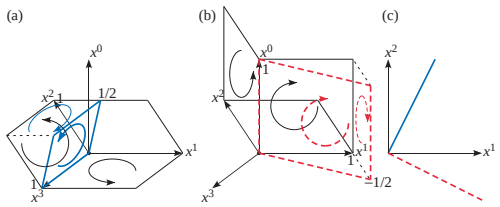

Fig. 2. Another set of faces of primal and dual grids based on Hodge duality: (a) primal face, (b) dual face, and (c) the projections on the x^1-x^2 plane.

satisfy (13). The projections of these faces on the x^1-x^2 plane in Fig. 2(c) show the orthogonality in the space is equivalent to that given by the Euclidean metric.

In materials, the metric is modified depending on the speed of light. To relate f to g, the dual grid is constructed in materials so as to satisfy:

$$S_{\mathrm{d}0j} = aS_{\mathrm{p}kl}/c_{\mathrm{r}}, S_{\mathrm{d}kl} = -ac_{\mathrm{r}}S_{\mathrm{p}0j}, (j = 1, 2, 3) \quad (15)$$
$$c_{\mathrm{r}} = 1/\sqrt{\varepsilon_{\mathrm{r}}\mu_{\mathrm{r}}} \quad (16)$$

where a is an arbitrary constant determining the size of S_{d}, (j, k, l) is a cyclic permutation of (1, 2, 3), and ε_{r} and μ_{r} are the specific permittivity and permeability. Thereby,

$$f = Zg/a \quad (17)$$

where $Z = \sqrt{\mu/\varepsilon}$ is the impedance.

The Hodge dual grid above gives a simple expression of the constitutive equation without permittivity and reluctivity matrices that are required by the Whitney elements [12], etc. However, the existence of the dual grid is not generally guaranteed for an arbitrary primal grid.

C. Explicit Time-Marching

For the space-time FI method to be as efficient as the conventional FDTD method, an explicit time-marching scheme is required. An explicit scheme is given as follows.

Fig. 3 presents a space-time grid projected on the x^0-x^1 plane in which the solid and dashed lines denote the faces of primal and dual grids. The projection on the x^0-x^1 plane allows the face direction to be represented by the straight arrows instead of the rotational arrows used in Figs. 1 and 2. The grid has three domains according to the time-step: (I) the domain with time-step Δx^0, (II) the domain with $\Delta x^0/2$, and (III) the domain connecting (I) and (II). For simplicity, ε and μ are assumed to be uniform and Δx^i $(i = 1, 2, 3)$ are uniformly set to unity; the time-step is assumed to be uniform along the x^2 and x^3 directions. Fig. 4 illustrates the primal and dual grids required in the connecting domain.

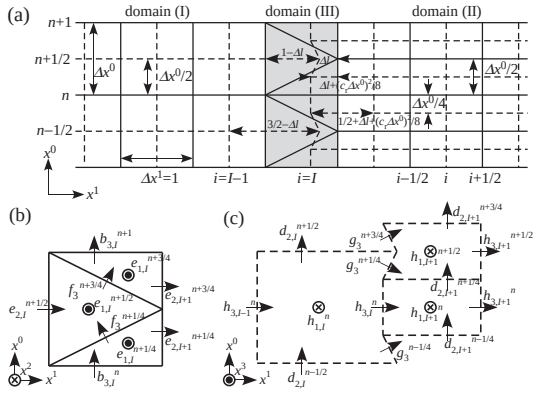

Fig. 3. The connection of domain (I) and (II): (a) primal and dual grids projected on the x^0-x^1 plane, (b) electromagnetic variables for the primal grid, and (c) electromagnetic variables for the dual grid.

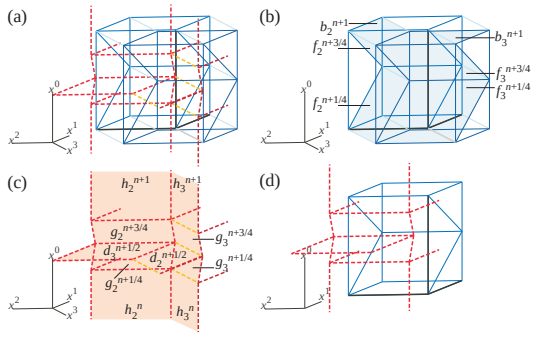

Fig. 4. Primal and dual grids in the connecting domain: (a) primal and dual grids, (b) primal grid, (c) dual grid, and (d) 3D grids for comparison.

In domain (I), d_m and e_m are updated as:

$$d^{n+1/2}_{m,i,j,k} = d^{n-1/2}_{m,i,j,k} + \boldsymbol{C}_{\mathrm{dm}}\boldsymbol{h}^{n}_{i,j,k},$$
$$e^{n+1/2}_{m,i,j,k} = c_{\mathrm{r}}Z\Delta x^0 d^{n+1/2}_{m,i,j,k}, (m = 1,2,3, i \le I-1). \quad (18)$$

In domain (II), d_m and e_m are updated as:

$$d^{n+1/4}_{m,i,j,k} = d^{n-1/4}_{m,i,j,k} + \boldsymbol{C}_{\mathrm{dm}}\boldsymbol{h}^{n}_{i,j,k},$$
$$e^{n+1/4}_{m,i,j,k} = (c_{\mathrm{r}}Z\Delta x^0/2) d^{n+1/4}_{m,i,j,k},$$
$$(i \ge I+1 \text{ for } m = 1 \text{ and } i \ge I+2 \text{ for } m = 2,3). \quad (19)$$

In connecting domain (III), d_m and e_m are updated as:

$$d^{n+1/4}_{1,I,j,k} = d^{n-1/4}_{1,I,j,k} + \boldsymbol{C}_{\mathrm{d1}}\boldsymbol{h}^{n}_{I,j,k},$$
$$e^{n+1/4}_{1,I,j,k} = (c_{\mathrm{r}}Z\Delta x^0/4) d^{n+1/4}_{1,I,j,k} \quad (20)$$
$$d^{n+1/4}_{m,I+1,j,k} = d^{n-1/4}_{m,I+1,j,k} + \boldsymbol{C}_{\mathrm{dm}}\boldsymbol{h}^{n}_{I+1,j,k},$$
$$e^{n+1/4}_{m,I+1,j,k} = \frac{c_{\mathrm{r}}Z\Delta x^0}{2} \frac{d^{n+1/4}_{m,I+1,j,k}}{\frac{1}{2} + \Delta l + \frac{(c_{\mathrm{r}}\Delta x^0)^2}{8}}, (m = 2,3) \quad (21)$$

where $0 < \Delta l < 1/2 - (c_{\mathrm{r}}\Delta x^0)^2/8$ (see Fig. 3(a)). In domain (III), variables $f^{n+1/4}_m$ and $g^{n+1/4}_m$ are defined as in Figs. 3 and 4, which are given as:

$$f^{n+1/4}_{2,j,k} = b^{n}_{2,I,j,k} + e^{n+1/4}_{3,I+1,j,k} - e^{n+1/4}_{1,I,j,k+1} + e^{n+1/4}_{1,I,j,k} \quad (22)$$
$$f^{n+1/4}_{3,j,k} = b^{n}_{3,I,j,k} - e^{n+1/4}_{2,I+1,j,k} + e^{n+1/4}_{1,I,j+1,k} - e^{n+1/4}_{1,I,j,k} \quad (23)$$
$$g^{n+1/4}_{m,j,k} = (c_{\mathrm{r}}\Delta x^0/4) f^{n+1/4}_{m,j,k}/Z, (m = 2,3). \quad (24)$$

Then d_m and e_m in domain (III) are given as (see Fig. 3(c)):

$$d^{n+1/2}_{1,I,j,k} = d^{n+1/4}_{1,I,j,k} + \boldsymbol{C}_{\mathrm{d1}}\boldsymbol{g}^{n+1/4}_{j,k},$$
$$e^{n+1/2}_{1,I,j,k} = (c_{\mathrm{r}}Z\Delta x^0/2) d^{n+1/2}_{1,I,j,k} \quad (25)$$
$$d^{n+1/2}_{2,I,j,k} = d^{n-1/2}_{2,I,j,k} + \boldsymbol{C}_{\mathrm{d2}}\boldsymbol{h}^{n}_{I,j,k} - g^{n-1/4}_{3,j,k} - g^{n+1/4}_{3,j,k},$$
$$d^{n+1/2}_{3,I,j,k} = d^{n-1/2}_{3,I,j,k} + \boldsymbol{C}_{\mathrm{d3}}\boldsymbol{h}^{n}_{I,j,k} + g^{n-1/4}_{2,j,k} + g^{n+1/4}_{2,j,k},$$
$$e^{n+1/2}_{m,I,j,k} = c_{\mathrm{r}}Z\Delta x^0 d^{n+1/2}_{m,I,j,k}/(3/2 - \Delta l), (m = 2,3). \quad (26)$$

In domain (II), b_m and h_m are updated as:

$$b^{n+1/2}_{m,i,j,k} = b^{n}_{m,i,j,k} - \boldsymbol{C}_{\mathrm{pm}}\boldsymbol{e}^{n+1/4}_{i,j,k}, (m = 1,2,3, i \ge I+1) \quad (27)$$

$$h^{n+1/2}_{m,i,j,k} = (c_{\mathrm{r}}\Delta x^0/2) b^{n+1/2}_{m,i,j,k}/Z,$$
$$(i \ge I+2 \text{ for } m = 1, i \ge I+1 \text{ for } m = 2,3) \quad (28)$$
$$h^{n+1/2}_{1,I+1,j,k} = \frac{c_{\mathrm{r}}\Delta x^0}{2Z}\Big[\frac{1}{2} + \Delta l + \frac{(c_{\mathrm{r}}\Delta x^0)^2}{16}\Big] b^{n+1/2}_{1,I+1,j,k}. \quad (29)$$

Then, $f^{n+3/4}_m$ and $g^{n+3/4}_m$ in domain (III) are (see Fig. 3(b)):

$$f^{n+3/4}_{2,j,k} = f^{n+1/4}_{2,j,k} - e^{n+1/2}_{3,I,j,k} - e^{n+1/2}_{1,I,j,k+1} + e^{n+1/2}_{1,I,j,k} \quad (30)$$
$$f^{n+3/4}_{3,j,k} = f^{n+1/4}_{3,j,k} + e^{n+1/2}_{2,I,j,k} + e^{n+1/2}_{1,I,j+1,k} - e^{n+1/2}_{1,I,j,k} \quad (31)$$
$$g^{n+3/4}_{m,j,k} = (c_{\mathrm{r}}\Delta x^0/4) f^{n+3/4}_{m,j,k}/Z, (m = 2,3). \quad (32)$$

Subsequently, d_m and e_m in domain (II) are updated similarly to (19) to obtain $d^{n+3/4}_{m,i,j,k}$ and $e^{n+3/4}_{m,i,j,k}$ ($i \ge I+1$ for $m = 1$ and $i \ge I+2$ for $m = 2,3$). Then, d_m and e_m in connecting domain (III) are updated as (see Figs. 3(c)):

$$d^{n+3/4}_{2,I+1,j,k} = d^{n+1/4}_{2,I+1,j,k} + h^{n+1/2}_{1,I+1,j,k} - h^{n+1/2}_{1,I+1,j,k-1} - h^{n+1/2}_{3,I+1,j,k} + g^{n+1/4}_{3,j,k} + g^{n+3/4}_{3,j,k},$$
$$d^{n+3/4}_{3,I+1,j,k} = d^{n+1/4}_{3,I+1,j,k} + h^{n+1/2}_{2,I+1,j,k} - g^{n+1/4}_{2,j,k} - g^{n+3/4}_{2,j,k} - h^{n+1/2}_{1,I+1,j,k} + h^{n+1/2}_{1,I+1,j-1,k},$$
$$e^{n+3/4}_{m,I+1,j,k} = \frac{c_{\mathrm{r}}Z\Delta x^0}{2} \frac{d^{n+3/4}_{m,I+1,j,k}}{\frac{1}{2} + \Delta l + \frac{(c_{\mathrm{r}}\Delta x^0)^2}{8}}, (m = 2,3) \quad (33)$$
$$d^{n+3/4}_{1,I,j,k} = d^{n+1/2}_{1,I,j,k} + \boldsymbol{C}_{\mathrm{d1}}\boldsymbol{g}^{n+3/4}_{j,k},$$
$$e^{n+3/4}_{1,I,j,k} = (c_{\mathrm{r}}Z\Delta x^0/4) d^{n+3/4}_{1,I,j,k}. \quad (34)$$

In domain (I), b_m and h_m are updated as:

$$b^{n+1}_{m,i,j,k} = b^{n}_{m,i,j,k} - \boldsymbol{C}_{\mathrm{pm}}\boldsymbol{e}^{n+1/2}_{i,j,k},$$
$$h^{n+1}_{m,i,j,k} = \frac{c_{\mathrm{r}}\Delta x^0}{Z} b^{n+1}_{m,i,j,k}, (m = 1,2,3, i \le I-1). \quad (35)$$

In domain (II), b_m and h_m are updated similarly to (27) and (28) to obtain $b^{n+1}_{m,i,j,k}$ and $h^{n+1}_{m,i,j,k}$; $h^{n+1}_{1,I+1,j,k}$ is given as:

$$h^{n+1}_{1,I+1,j,k} = \frac{c_{\mathrm{r}}\Delta x^0}{2Z}\Big[\frac{1}{2} + \Delta l + \frac{(c_{\mathrm{r}}\Delta x^0)^2}{8}\Big] b^{n+1}_{1,I+1,j,k}. \quad (36)$$

In domain (III), b_m and h_m are updated as (see Fig. 3(b)):

$$b^{n+1}_{1,I,j,k} = b^{n}_{1,I,j,k} - \boldsymbol{C}_{\mathrm{p1}}\boldsymbol{e}^{n+1/2}_{I,j,k} \quad (37)$$
$$h^{n+1}_{1,I,j,k} = \frac{c_{\mathrm{r}}\Delta x^0}{Z}\Big[\frac{3}{2} - \Delta l - \frac{3(c_{\mathrm{r}}\Delta x^0)^2}{32}\Big] b^{n+1}_{1,I,j,k} \quad (38)$$
$$b^{n+1}_{2,I,j,k} = f^{n+3/4}_{2,I,j,k} + e^{n+3/4}_{3,I+1,j,k} - e^{n+3/4}_{1,I,j,k+1} + e^{n+3/4}_{1,I,j,k} \quad (39)$$
$$b^{n+1}_{3,I,j,k} = f^{n+3/4}_{3,I,j,k} - e^{n+3/4}_{2,I+1,j,k} + e^{n+3/4}_{1,I,j+1,k} - e^{n+3/4}_{1,I,j,k} \quad (40)$$
$$h^{n+1}_{m,I,j,k} = (c_{\mathrm{r}}\Delta x^0/2) b^{n+1}_{m,I,j,k}/Z, (m = 2,3). \quad (41)$$

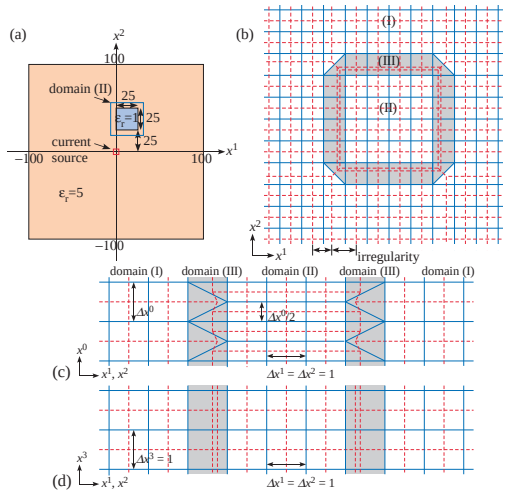

Fig. 5. Geometry of application example and space-time grid: (a) source and domain (II), (b) space-time grid projected on the x^1-x^2 plane, (c) projected on the x^0-$x^1(x^2)$ plane, and (d) projected on the $x^1(x^2)$-x^3 plane; solid line: primal grid, dashed line dual grid; the number of elements does not correspond to the simulations shown in Fig. 7.

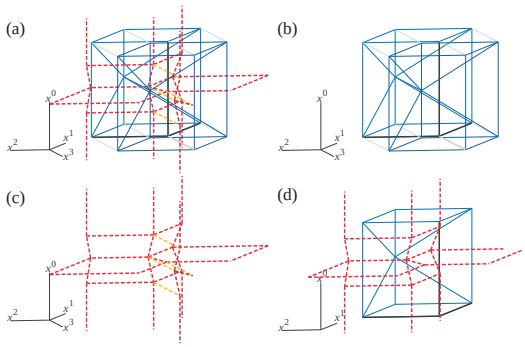

Fig. 6. Primal and dual grids at the corner of domain (III): (a) primal and dual grids, (b) primal grid, (c) dual grid, and (d) 3D grids for comparison.

III. Application to Wave Computation

Wave propagation induced by an electric current source is analyzed to examine the space-time FI method. The electric current source with a normalized frequency of 0.05 is located as shown in Fig. 5(a). Figs. 5(b), (c) and (d) present a space-time grid in which the solid and dashed lines denote primal and dual grids. Domains (I) and (II) have uniform time-steps Δx^0 and $\Delta x^0/2$, which are connected by domain (III). Fig. 6 illustrates the primal and dual grids required at the corner of domain (III). An explicit time-marching scheme is developed for this space-time grid. For simplicity, the permeability is set uniformly to unity by normalization: the permittivity is set to 5 in domains (I) and (III) whereas the permittivity is unity in a part of domain (II) as shown in Fig. 5(a). The spatial grid sizes Δx^1 and Δx^2 are set to unity in domains (I) and (II), and Δx^3 is uniformly set to unity in the spatial domain size of 160^3. The time step Δx^0 is unity in domain (I). Fig. 7(a) portrays a distribution of B_z at x^0 = 200 given by the space-time FI method. For comparison, Fig. 7(b) depicts the distribution obtained using the conventional FDTD method with the same uniform spatial grid and time-step as in domain (II), which is restricted by the smallest permittivity. The computation time

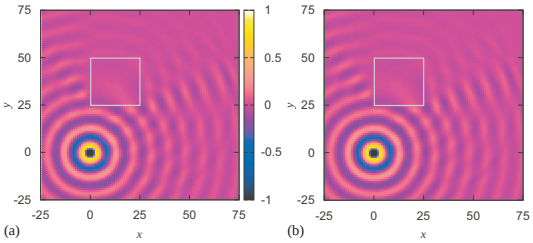

Fig. 7. Distributions of B_z: (a) space-time FI method and (b) FDTD method.

executed on Intel Core 2 Duo E6400 was 305 s for the FDTD method whereas it was reduced to 152 s for the space-time FI method because of the large time-step in domain (I). The space-time FI method yields the correct wave propagation; the maximum discrepancy of $\boldsymbol{B}$ between the two methods is 3.1 %, where the discrepancy is normalized by the maximal $|\boldsymbol{B}|$. The discrepancy is caused by the nonuniform grids [10] including the irregularity indicated in Fig. 5(b). The discrepancy can be reduced by the use of fine spatial grid compared with the wavelength. When the normalized frequency is changed to 0.1 or 0.025, the discrepancy becomes 6.2 % or 1.6 %, respectively, owing to the wavelength change. The numerical instability is not observed even after $x^0 = 10^4 \Delta x^0$.

IV. Conclusion

A Hodge dual grid based on the Lorentz metric is proposed to obtain a simple constitutive relationship for electromagnetic variables in the 4D space-time finite integration method. An explicit time-marching scheme was presented to achieve more efficient computation than the conventional FDTD method.

References

[1] K. S. Yee, "Numerical solution of initial boundary value problems involving Maxwell's equations in isotropic media," *IEEE Trans. Antennas Propagat.*, vol. 14, pp. 302-307, May 1966.
[2] T. Weiland, "Time domain electromagnetic field computation with finite difference methods," *Int. J. Numer. Model.*, vol. 9, pp. 295-319, 1996.
[3] I. E. Lager, E. Tonti, A.T. de Hoop, G. Mur, and M. Marrone, "Finite formulation and domain-integrated field relations in electromagnetics – a synthesis," *IEEE Trans. Magn.*, vol. 39, pp. 1199-1202, May 2003.
[4] M. W. Chevalier, R.J. Luebbers, and V.P. Cable, "FDTD local grid with material traverse," *IEEE Trans. Antennas Propagat.*, vol. 45, pp. 411-412, March 1997.
[5] P. Thoma and T. Weiland, "A consistent subgridding scheme for the finite difference time domain method," *Int. J. Numer. Model.*, vol. 9, pp. 359-374, 1996.
[6] A. Einstein, "Zur Elektrodynamik bewegter Körper," *Ann. Phys.*, vol. 17, pp. 891-921, 1905.
[7] A.J. Butler and Z.J. Cendes, "Space-time finite elements derived by convolution for the efficient solution of transient eddy current problems," *IEEE Trans. Magn.*, vol. 24, pp. 2688-2690, Nov. 1988.
[8] T. Renyuan, L. Feng, L. Yan and C. Xiang, "Analysis of transient nonlinear eddy current fields by space-time finite element method," *IEEE Trans. Magn.*, vol. 34, pp. 2577-2580, Sept. 1998.
[9] S. Gyimóthy, A. Vágvölgyi, and I. Sebestyén, "Application of optimally distorted finite elements for field calculation problems of electromagnetism," *IEEE Trans. Magn.*, vol. 38, pp. 365-368, March 2002.
[10] T. Matsuo, "Electromagnetic field computation using space-time grid and finite integration method," *IEEE Trans. Magn.* vol. 46, pp. 3241-3244, Aug. 2010.
[11] T. Frankel, *The Geometry of Physics: An Introduction*, Cambridge University Press: Cambridge, 2004.
[12] A. Bossavit, *Computational Electromagnetism: Variational Formulations, Complementarity, Edge Elements*, Academic Press: Boston, 1998.